THE JOURNAL OF BIOLOGICAL CHEMISTRY
Vol. 280, No. 4, Issue of January 28, pp. 2826–2830, 2005

Printed in U.S.A.

A Dynamic Zinc Redox Switch*[S]

Received for publication, November 5, 2004, and in revised form, November 15, 2004
Published, JBC Papers in Press, November 17, 2004, DOI 10.1074/jbc.C400517200

Ana Mirela Neculai‡§¶, Dante Neculai‡§¶, Christian Griesinger‡, Julia A. Vorholt‖, and Stefan Becker‡¶**

From the ‡Department for NMR-based Structural Biology, Max Planck Institute for Biophysical Chemistry, Am Fassberg 11, 37077 Göttingen, Germany and ‖Laboratoire des Interactions Plantes Microorganismes, INRA/CNRS, 31326 Castanet-Tolosan, France

The crystal structures of glutathione-dependent formaldehyde-activating enzyme (Gfa) from *Paracoccus denitrificans*, which catalyzes the formation of *S*-hydroxymethylglutathione from formaldehyde and glutathione, and its complex with glutathione (Gfa-GTT) have been determined. Gfa has a new fold with two zinc-sulfur centers, one that is structural (zinc tetracoordinated) and one catalytic (zinc apparently tricoordinated). In Gfa-GTT, the catalytic zinc is displaced due to disulfide bond formation of glutathione with one of the zinc-coordinating cysteines. Soaking crystals of Gfa-GTT with formaldehyde restores the holoenzyme. Accordingly, the displaced zinc forms a complex by scavenging formaldehyde and glutathione. The activation of formaldehyde and of glutathione in this zinc complex favors the final nucleophilic addition, followed by relocation of zinc in the catalytic site. Therefore, the structures of Gfa and Gfa-GTT draw the critical association between a dynamic zinc redox switch and a nucleophilic addition as a new facet of the redox activity of zinc-sulfur sites.

The redox activity of sulfur ligands in zinc sites, known as zinc redox switch, is a basic principle to control protein function in redox biology (1). It involves the reversible oxidation and reduction of the cysteine ligands bound to the redox-inert zinc ion. The concept has been developed and probed to explain mechanisms to control zinc homeostasis in the cell, to induce conformational changes in proteins resulting in their active, functional form, and in activation or inactivation of enzymes (2). The zinc redox switch mechanism is linked to the binding and release of zinc and involves oxidants such as nitric oxide and GSSG (3–5).

A generally accepted model for the zinc redox switch involving glutathione is the release of zinc upon disulfide bond formation between a glutathione and a zinc-coordinating thiol, known as the "cysteine switch" mechanism (6). To gain new insights into this partnership we advocate in the following the example of a formaldehyde-converting zinc enzyme that uses glutathione as co-substrate. This zinc enzyme employs a dynamic Zn-S redox switch, crucial to an essentially nucleophilic addition. This means that a cysteine switch step takes place during each turnover of the enzyme. On the contrary, zinc redox switches investigated thus far precede as singular events subsequent reactions, hence having a trigger function for these reactions without being mechanistically involved in them any more.

Because of its toxic nature, formaldehyde needs to be efficiently metabolized. In most organisms this is achieved through the GSH-linked oxidation pathway. Its first step is the formation of the *S*-hydroxymethylglutathione adduct by reaction of formaldehyde with the SH group of glutathione (7). Subsequently, *S*-hydroxymethylglutathione is oxidized by glutathione-dependent formaldehyde dehydrogenase, a class III alcohol dehydrogenase (8). Finally *S*-formylglutathione hydrolase regenerates glutathione and releases formate (9), which can be oxidized in some organisms to carbon dioxide.

The adduct formation as the first step of the glutathione-linked formaldehyde oxidation is usually an uncatalyzed reaction *in vivo* (10). However, in the methylotrophic α-proteobacterium *Paracoccus denitrificans,* an enzyme was identified that allows for an increased turnover compared with the uncatalyzed reaction (11). This enzyme, a 21-kDa protein, was named glutathione-dependent formaldehyde-activating enzyme (Gfa).[1] Gfa shows high sequence homology to putative proteins from a number of proteobacteria (see supplemental Fig. 1) (11). It contains clustered cysteine residues, opening the possibility that the protein might contain zinc binding sites. This raised the questions of whether and, if so, how a catalytic zinc center might be functionally involved in the formation of *S*-hydroxymethylglutathione.

To address these questions, we determined the crystal structures of both unliganded and glutathione-bound enzyme (Gfa-GTT), as well as the structure from crystals of Gfa-GTT soaked with formaldehyde. The structure of Gfa encloses two zinc sites and turns out to have a new fold. Soaking crystals of this intermediate with formaldehyde results in the reconstitution of the holoenzyme structure. Based on these observations, we suggest a mechanism for the nucleophilic addition that places a dynamic zinc redox switch at the core of the enzymatic reaction.

EXPERIMENTAL PROCEDURES

Protein Expression and Purification—The gene *gfa* from *P. denitrificans* was amplified by PCR from genomic DNA and cloned into a modified pET16b vector containing a TEV cleavage site. This expression construct was transformed into the *Escherichia coli* strain

* The costs of publication of this article were defrayed in part by the payment of page charges. This article must therefore be hereby marked "*advertisement*" in accordance with 18 U.S.C. Section 1734 solely to indicate this fact.

[S] The on-line version of this article (available at http://www.jbc.org) contains supplemental material.

The atomic coordinates and structure factors (codes 1X6M and 1XA8) have been deposited in the Protein Data Bank, Research Collaboratory for Structural Bioinformatics, Rutgers University, New Brunswick, NJ (http://www.rcsb.org/).

§ These authors contributed equally to this work.

¶ Supported by Max-Planck-Gesellschaft and Grant BE2345 from the Deutsche Forschungsgemeinschaft.

** To whom correspondence should be addressed. Tel.: 49-551-201-2222; Fax: 49-551-201-2202; E-mail: sabe@nmr.mpibpc.mpg.de.

[1] The abbreviations used are: Gfa, glutathione-dependent formaldehyde-activating enzyme; Gfa-GTT, Gfa-glutathione complex; Gfa-GTT-FOR, Gfa-GTT complex soaked with formaldehyde; r.m.s.d., root mean square deviation; SAD, single-wavelength anomalous dispersion.

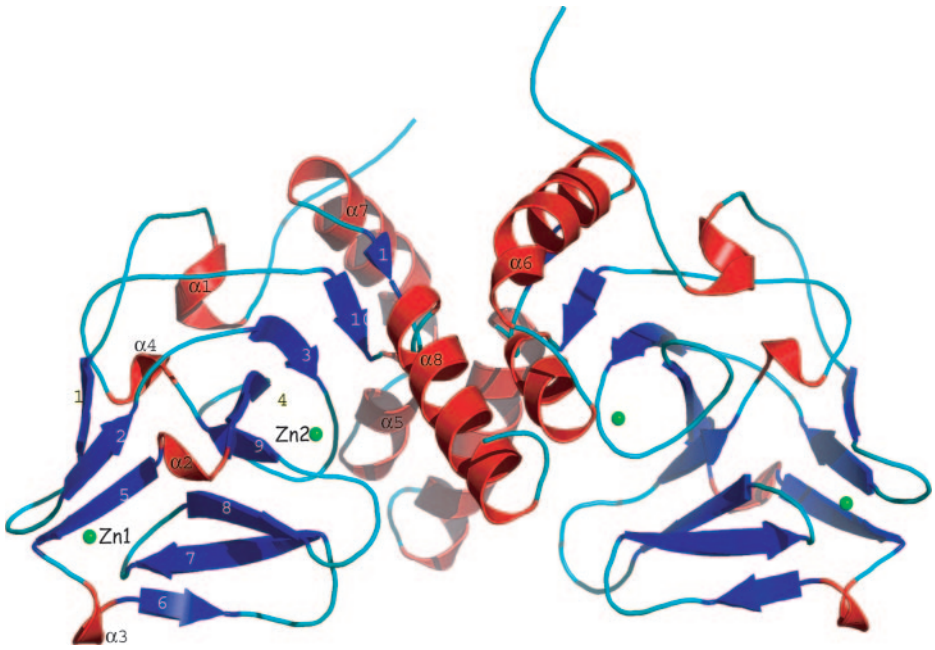

FIG. 1. **Ribbon representation of the Gfa dimer.** The molecules are colored according to their secondary structures: helices are in *red* (α1, α7, α8), including the 3_{10} helices (α2, α3, α4, α6 (the latter is not visible within the same monomer and is assigned in the other monomer); the extended eight-stranded β-sheet (β6, β7, β8, β9, β4, β3, β10, β10, β11) sandwiched with the triple-stranded β-sheet (β1, β2, β5) is in *blue*.

BL21(DE3). Protein expression was carried out at 23 °C after induction with 0.5 mM isopropyl-1-thio-β-D-galactopyranoside. Cells from 750 ml of expression culture were harvested 8 h after induction and resuspended in 40 ml of lysis buffer (20 mM Tris, pH 7.9, 0.5 M NaCl, 10 mM imidazole, 0.5 mM phenylmethylsulfonyl fluoride). The His_{10}-tagged Gfa fusion protein was purified by standard methods using nickel-nitrilotriacetic acid resin and TEV protease for cleaving of the His_{10} tag. The final purification was performed by gel filtration on a Superdex 75HR 3/10 column, which was also used to transfer the protein to the final buffer for crystallization and storage (20 mM HEPES, pH 7.0, 100 mM NaCl, 0.5 mM phenylmethylsulfonyl fluoride). The final yield of purified Gfa was typically 30 mg from 750 ml of culture. For crystallization, the purified Gfa was concentrated to 9 mg/ml. Se-Met-labeled Gfa was overexpressed in minimal media supplemented with seleno-methionine according to the EMBL protein expression group (embl-heidelberg.de) and purified according to the established protocol.

Crystallization and Data Collection—Crystals of *P. denitrificans* Gfa were obtained using vapor diffusion by mixing 2 μl of concentrated protein solution with 2 μl of reservoir solution (2–2.1 M $(NH_4)_2SO_4$, 4% polyethylene glycol 400, and 0.1 M HEPES, pH 7.4). They grew within 3–4 days as overlapping plates with dimensions of 0.5 × 0.3 × 0.05 mm. For crystallization of the Gfa-glutathione complex, the reduced form of L-glutathione (10 mM, Sigma) and 5 mM β-mercaptoethanol were added to the reservoir solution. The crystals were cryoprotected by transferring them into a solution consisting of crystallization buffer and 10% glycerol prior to freezing in liquid nitrogen. To investigate the reaction with formaldehyde, crystals of Gfa-GTT were soaked in a fresh solution containing crystallization buffer, 10% glycerol, and 50 mM formaldehyde for 3–5 min, flash-frozen, and stored under liquid nitrogen. Data were collected for Gfa at Advanced Light Source (X6S, Q210 CCD detector) and for Gfa-GTT as well as Gfa-GTT crystals that have been soaked with formaldehyde (Gfa-GTT-FOR),[2] at DESY Hamburg (BW6, Mar CCD detector), respectively. Data were processed using the program XDS (12). Statistics for data collection and processing are summarized in supplemental Table I.

Structure Determination and Refinement—The Gfa structure has been solved by SAD phasing from monoclinic crystals grown using protein incorporating labeled Se-Met. Selenium positions have been found using SOLVE-2.6 based on selenium atoms refinement against anomalous differences at 75–3.8 Å (13). RESOLVE was used to extend the resolution to native data, to calculate initial experimental electron density maps, and to obtain the initial model. Further model building was carried out with XtalView and ARP/wARP (14). Refinement was done at all stages with REFMAC5 (15). Water molecules were added with ARP/wARP and checked. The secondary structure has been assigned using the program DSSP (16)

The structures of the complexes were solved by molecular replacement with the program MOLREP (17) using the structure of Gfa as the search model. After manual model building in the catalytic zinc site, including placement of GTT from the respective REFMAC5 libraries, refinement was done by REFMAC5 similar to the procedure for the holoenzyme. The model geometry was inspected with PROCHECK (18). The molecular figures were generated with Pymol and DINO.

RESULTS

Overall Structure and Zinc Binding Sites—The structure of Gfa was solved to a resolution of 2.35 Å by SAD (19) (supplemental Table I). The 4 monomers in the asymmetric unit clearly form 2 homodimers. The size of the dimer interface is ~890 Å^2 and is equally made by polar and hydrophobic interactions, whereas the interface between the two dimers covers only 60 Å^2. Dimer formation in solution was confirmed by gel filtration chromatography and dynamic light scattering measurements (data not shown). Because no major difference was observed between the 2 dimers (r.m.s.d. 0.59 Å for the Cα atoms), we have focused our description on a single dimer (Fig. 1). Gfa forms a globular structure with a new fold (no matches with the DALI server (20)). Thus Gfa and its so far identified sequence orthologs (supplemental Fig. 1) form a new structural family.

The main topological feature of this structure is an extremely twisted mixed eight-stranded β-sheet (see supplemental Fig. 2). Within this β-sheet, the strands β_8, β_9, and β_4 form a sandwich with another triple stranded mixed β-sheet (β_5, β_2, β_1). The interconnection between the sheets is mediated by four 3_{10} helices (α_2, α_3, α_4, α_6) and two α-helices (α_5, α_7). Helices α_5 and α_7 form a small antiparallel bundle and are packing against helix α_8 of the opposite monomer, thus constituting a major portion of the interface between the monomers. The structure of each monomer is completed by another short α-helix, α_1 (at the N termini), which faces α_5, α_6, and α_8 (at the C termini). The novelty of this $3_{10}/\beta$ structure resides in the exclusive combination of antiparallel β-sheets with a relatively high number of 3_{10} helices (4), a rare occurrence in known protein structures because of unfavorable energetics. The sandwich arrangement of the β-strands is further buttressed by a tetrahedral zinc coordinated by the side chains of Cys-33, Cys-35, Cys-101, and Cys-104 (see supplemental Fig. 3). It appears

[2] Because of the very high similarity with the Gfa structure, the coordinates and the structure factors for the Gfa-GTT-FOR crystals were not deposited in the Protein Data Bank but are available upon request.

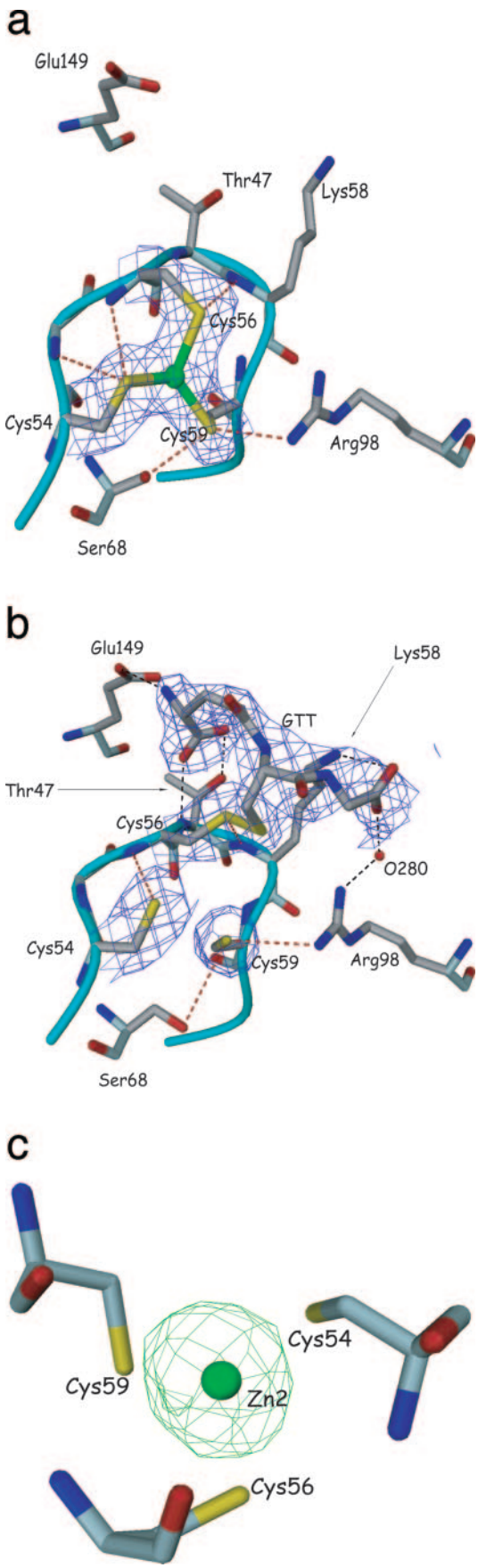

FIG. 2. *a* and *b*, view of the catalytic site of Gfa (*a*) and Gfa-GTT (*b*) including the H-bonding network (*dotted lines*) in which the zinc-coordinating thiol groups are involved. The residues involved in Zn2 (*a*) and GTT (*b*) binding are labeled accordingly. The representation also contains the electron density at 1σ level in the $2F_o - F_c$ map for the catalytic zinc and the Cys residues in Gfa (*a*) and for Cys residues and GTT in Gfa-GTT (*B*). To evaluate the changes upon GTT coordination, we chose similar perspectives of the active site. Numbering of the residues is according to the expression construct that contains three additional amino acids at the N terminus. *c*, electron density contoured at 3σ level in the $F_o - F_c$ map (in *green*) at the catalytic site of Gfa-GTT soaked with formaldehyde.

that this zinc atom has only a structural role. A second zinc ion stabilizes a large hairpin loop that connects β_3 and β_4 via residues Cys-54, Cys-56, and Cys-59 (Fig. 2*a*). The presence of zinc as the coordinated metal in Gfa has been proven by its absorption edge in the x-ray fluorescence spectrum (data not shown). Although the structural zinc is fully occupied in all monomers, the occupancy of the second zinc site was refined to 0.6. Because of its apparently labile coordination environment, this zinc site was a candidate for the catalytic function of Gfa. Similar examples, as far as the coordination sphere is concerned, have been reported (21). The three cysteine residues create a nearly planar arrangement with the zinc, resulting in S-Zn-S angles of ~ 120°. Electron density of water as a fourth ligand could not be identified. The nearest water molecule is 4.2 Å away from the catalytic site, and the orientation does not comply with tetrahedral geometry. The distance between the zinc ions in the monomers is 19.6–19.9 Å. Structurally there are no indications for functional interactions between them.

Although the resolution of the structure does not allow definite statements about the type of coordinated cysteines (as thiols or thiolates) at the catalytic zinc site, the involvement of the sulfur atoms in a network of H bonds is important in defining its mechanistic aspects. Hence, the three Cys side chains are at donor-acceptor distances of 3.1–3.7 Å (see supplemental Table II) with the main chain amides of Lys-58, Cys-56, and Gly -55 and the Nη2 of Arg-98, as well as with the hydroxyl group of Ser-68 (Fig. 2*a*). The existence of a so-called "outer coordination sphere" that contains Arg and Ser biases us toward the stabilization of thiolate moieties with lowered pK_a (22).

Glutathione Binding—To investigate the glutathione interaction with the presumed catalytic zinc center, Gfa was crystallized with an excess of reduced glutathione (1:20 (mol/mol) Gfa:GTT). In this structure glutathione formed a disulfide bond to Cys-56, completely displacing the catalytic zinc (Fig. 2*b*). In all four monomers the electron density for glutathione is well defined (Fig. 2*b*), whereas density for the displaced zinc could not be identified anywhere near the catalytic site. There are no major conformational differences among the amino acids forming the binding pocket of glutathione except for Cys-56, in which the side chain reorients to bridge to the cysteinyl residue of glutathione, and for Lys-58, in which the side chain anchors the glutathione by forming a salt bridge with the glycinyl moiety of glutathione (Fig. 2*b*). The other key residues for glutathione binding are functionally conserved within the group of Gfa orthologs and other glutathione-binding proteins (Fig. 2*b*) (23). The glutathione pocket seems to be preexistent in the monomer, the dimer formation having probably only a stabilizing role. The H-bonding network around thiolate moieties described for Gfa is maintained also for Gfa-GTT (Fig. 2, *a* and *b*).

The overall location of glutathione, very exposed to the solvent region, is reminiscent of the structures of glutathione transferases (24), but except for the cysteine-glutathione disulfide bridge, no functional connotations can be drawn between them.

The Gfa-Glutathione Complex Reacts with Formaldehyde—When crystals of Gfa-GTT were soaked with formaldehyde, the $F_o - F_c$ difference map allowed the identification of clear pos-

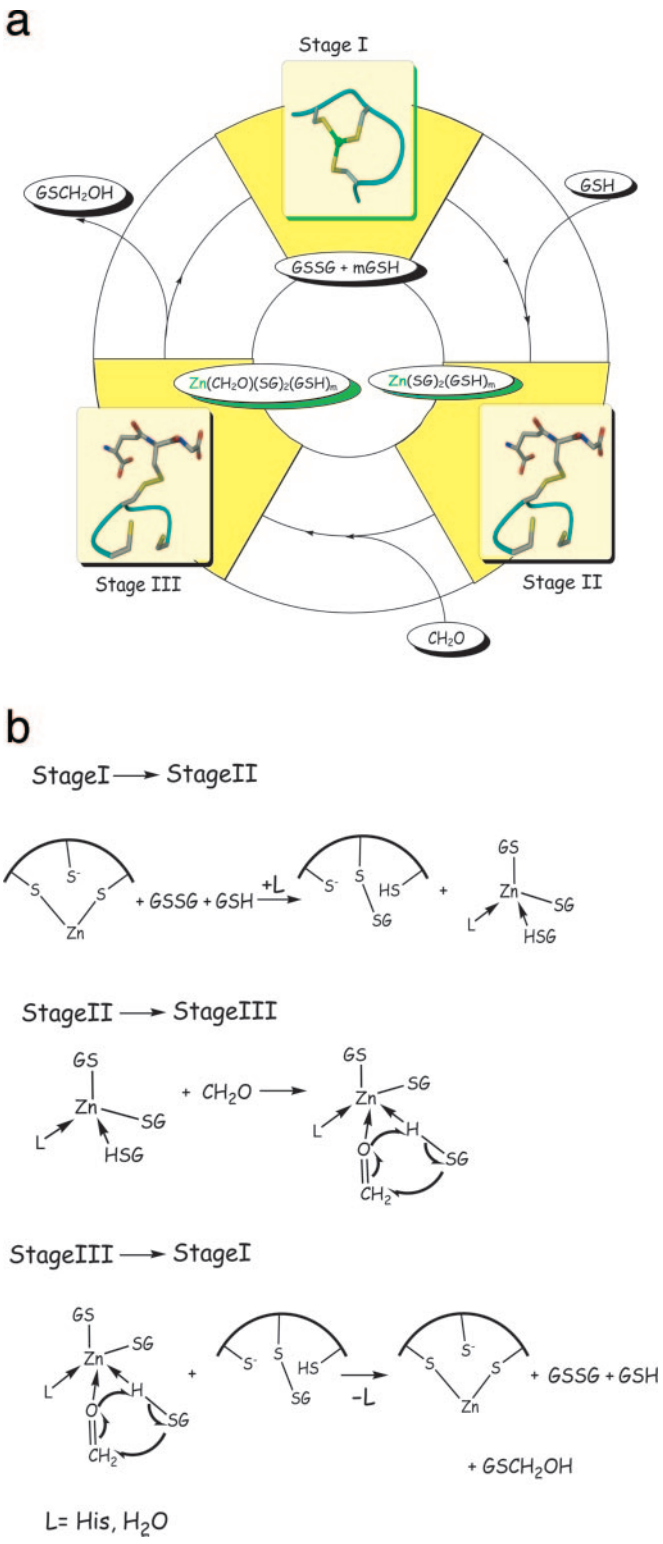

FIG. 3. *a*, time-resolved, three-stage catalytic cycle of Gfa. The *outer circle* presents the two structurally characterized intermediates that are associated to the postulated small molecule intermediates (*inner circle*). *Stage I* represents the initial situation, with Gfa in the presence of oxidized and reduced glutathione. *Stage II* represents the products of the reaction between Gfa and glutathione: the intermediate with dislocated zinc (Gfa-GTT) and the Zn-glutathione complex of unknown composition (m = 1 or 2), which subsequently scavenges formaldehyde. In this zinc complex the carbonyl bond of formaldehyde, as well as the sulfinyl bond of reduced glutathione, is polarized and thus activated for the final nucleophilic addition. For simplicity, only one variable has been chosen to describe the coordination number of zinc, taking into account the multiplicity of ligands (L) possibly bound to it (*e.g.* His, H_2O). The whole ensemble (*Stage III*) undergoes the transformation back to Stage I with concomitant release of *S*-hydroxymethylglutathione. *b*, schematic representation of the proposed reactions occurring at all stages of the catalytic pathway for m = 1. The complexes involved and all of the reactions are formulated taking into account the oxidation state of +2 for zinc and the electroneutrality principle.

itive electron density at the catalytic site, attributable to a zinc atom (Fig. 2*c*). Further refinement resulted in a structure that was very similar to the structure of the holoenzyme (r.m.s.d. 0.32 Å). The recoordination of zinc strongly indicates a functional connection between Gfa-GTT and subsequent adduct formation. Thus Gfa-GTT must be an active intermediate of the catalytic cycle, and the catalytic zinc, despite its dislocation in the Gfa-GTT structure, still has to be retained in the protein near the catalytic site. An interesting feature of the Gfa structure, which fits this requirement, is a number of His residues (His-32, -50, -52, -107, -117, and –126). These residues, conserved for the whole Gfa family (see supplemental Fig. 4), are positioned relatively close to the active site (8–12 Å) and form a lining of the two wide-open channels connecting the two faces of the active site to the surface of the protein. Therefore the conserved His residues might function as a net keeping the released zinc in the neighborhood of the catalytic center, thus preventing its complete dissociation from the protein. Studies have shown that the ternary Zn-GSH-histidine complexes are readily formed and might be involved in zinc transport (25).

DISCUSSION

The structural identification of the Gfa-GTT intermediate combined with the inspection of the structure of Gfa allow formulating a hypothetical coupled reaction mechanism (Fig. 3). According to this mechanism it is actually the oxidized form of glutathione (GSSG) that reacts with Cys-56 to form the disulfide-bonded Gfa-GTT intermediate, in which zinc cannot be located either within or outside of the catalytic site.

Interestingly, the longest H-bond within the network of H-bonds involving the cysteines at the catalytic site is the one of Cys-56 to the main chain amide of Lys-58 (3.6–3.8 Å). Hence, Cys-56 is the least stabilized, relative to the other two cysteines by coordination to zinc, and thus energetically is most suitable to react with glutathione.

It can be hypothesized that the displaced zinc is coordinated to the reduced form of glutathione, because zinc is always associated *in vivo* with another cellular ligand and is never transferred as the free zinc ion (26). The presence of other ligands like water and possibly histidine in the zinc coordination sphere cannot be excluded. We postulate that this zinc complex, for which the exact stoichiometry is unknown at this stage, acts as a scavenger for the formaldehyde present in solution (Fig. 3, *Stage II* → *Stage III*). This would provide an explanation for another previously proposed role of Gfa as a formaldehyde scavenger (11). In this mixed complex the carbonyl bond of formaldehyde as well as the sulfinyl bond of reduced glutathione are polarized and thus activated for the final nucleophilic addition, resulting in the formation of *S*-hydoxymethylglutathione, the relocation of zinc in the catalytic site, and the regeneration of oxidized glutathione. The oxidized glutathione can be fed back into the catalytic cycle (Fig. 3, *Stage III* → *Stage I*).

Redox activity of sulfur ligands has been recognized as an important feature of zinc proteins, creating an oxidoreductive environment in which the ligands, but not the metal, are oxidized and reduced with concomitant release and binding of zinc (1, 4). It was also found in other proteins, that the presence of a redox agent such as glutathione influences the zinc transfer, with the ratio of reduced and oxidized glutathione playing a critical role in the complete displacement of zinc (27).

The displacement of zinc by binding of glutathione to a cysteine residue of the catalytic site turns the catalytic zinc center into a highly dynamic zinc redox switch, where zinc moves in a ping-pong fashion between its coordination site and a dislocated state forward and backward. In the dislocated state zinc exerts its actual catalytic function by activating coordinated formaldehyde and glutathione for the nucleophilic addition. Thus a dynamic zinc redox switch actually serves as the piston for the catalyzed nucleophilic addition. The perpetual large motions of zinc, which are implied in this mechanism, might be the rate-limiting step of the reaction and the reason for the low turnover number of Gfa. It has also been shown in the past that this reaction is strongly pH-dependent (11). The involvement of the glutathione redox system, the ratio of oxidized and reduced glutathione being pH-dependent, delivers an explanation for this observation. The dimensions of the catalytic cleft easily allow the accommodation of a number of glutathione molecules, an essential requirement for the postulated mechanism (see supplemental Fig. 5).

An alternative explanation for the activity of Gfa would be a mechanism similar to the one of alkyltransferases, such as MtaA or betaine-homocysteine *S*-methyltransferase (28, 29). The postulated role of zinc in these enzymes is that of a Lewis acid that binds the thiol substrates as thiolates and thus activates the thiol group to be alkylated. In the light of this mechanism the Gfa-GTT substrate would have to be considered an oxidative artifact of our crystallization conditions; but the fact that zinc is recoordinated upon the reaction of Gfa-GTT with formaldehyde clearly demonstrates that Gfa-GTT is a central intermediate of the nucleophilic addition catalyzed by Gfa. Therefore a mechanism similar to that of the alkyltransferases seems improbable.

Zinc redox switches described so far are single turnover events. For example, in the chaperone Hsp33 of *E. coli*, activation by displacement of zinc results in the formation of two intramolecular disulfide bonds and refolding of the monomeric protein, which can then dimerize and thus create the hydrophobic surface essential for functioning as a chaperone in protein folding (30, 31). In cellulose synthase, dimerization of the subunits occurs through the intermolecular disulfide bond formation after zinc release (32). Also in enzymes, single turnover displacement or binding of zinc has been found to inactivate or trigger enzyme activity. In betaine-homocysteine *S*-methyltransferase, the zinc displacement is followed by formation of a disulfide bond between two of three cysteines (29), resulting in inactivation. Zinc-replete enzyme is reactivated. In NO synthase, the release of the zinc bridging the two monomers through oxidation of its thiolate ligands causes uncoupling of NO synthesis (33). But even in this case there is no highly dynamic redox switch operating as found for Gfa. In contrast the mechanism of zinc release in Gfa is intrinsically a multiturnover event, because the formation of each single *S*-hydroxymethylglutathione molecule is concomitant with a dislocation and relocation cycle of zinc at the catalytic site.

In essence, the combined structures of the Gfa holoenzyme, its glutathione-bound form, and the structure obtained upon soaking Gfa-GTT crystals with formaldehyde allow for the first time an insight into a dynamic zinc redox switch and deliver the first structural proof of this redox principle. It remains to be seen whether this dynamic redox switch is confined to the new structural family of proteobacterial proteins to which Gfa belongs or whether it might also be identified in enzymes from other kingdoms of life.

Acknowledgments—We thank Prof. G. M. Sheldrick for valuable support and advice and H.-W. Adolph, E. Cedergren, J. Stubbe, and R. Thauer for critical reading of the manuscript. We are grateful to G. Bourenkov and C. Schulze-Briese for support with data collection.

REFERENCES

1. Maret, W. (2004) *Biochemistry* **43,** 3301–3309
2. Vallee, B. L., and Falchuk, K. H. (1993) *Physiol. Rev.* **73,** 79–118
3. Maret, W. (1995) *Neurochem. Int.* **27,** 111–117
4. Maret, W., and Vallee, B. L. (1998) *Proc. Natl. Acad. Sci. U. S. A.* **95,** 3478–3482
5. Maret, W. (1994) *Proc. Natl. Acad. Sci. U. S. A.* **91,** 237–241
6. Springman, E. B., Angleton, E. L., Birkedal-Hansen, H., and Van Wart, H. E. (1990) *Proc. Natl. Acad. Sci. U. S. A.* **87,** 364–368
7. Mason, R. P., Sanders, J. K., Crawford, A., and Hunter, B. K. (1986) *Biochemistry* **25,** 4504–4507
8. Sanghani, P. C., Bosron, W. F., and Hurley, T. J. (2002) *Biochemistry* **41,** 15189–15194
9. Harms, N., Ras, J., Reijnders, W. N., van Spanning, R. J., and Stouthamer, A. H. (1996) *J. Bacteriol.* **178,** 6296–6299
10. Gutheil, W. G., Kasimoglu, E., and Nicholson, P. C. (1997) *Biochem. Biophys. Res. Commun.* **238,** 693–696
11. Goenrich, M., Bartoschek, S., Hagemeier, C. H., Griesinger, C., and Vorholt, J. A. (2002) *J. Biol. Chem.* **277,** 3069–3072
12. Kabsch, W. (1993) *J. Appl. Crystallogr.* **26,** 795–800
13. Terwilliger, T. C., and Berendzen, J. (1999) *Acta Crystallogr. Sect. D Biol. Crystallogr.* **55,** 849–861
14. Lamzin, V. S., and Wilson, K. S. (1993) *Acta Crystallogr. Sect. D Biol. Crystallogr.* **49,** 129–147
15. Murshudov, G. N., Vagin, A. A., and Dodson, E. (1997) *Acta Crystallogr. Sect. D* **53,** 240–255
16. Kabsch, W., and Sander, C. (1983) *Biopolymers* **22,** 2577–2637
17. Vagin, A. A., and Teplyakov, A. (1997) *J. Appl. Crystallogr.* **30,** 1022–1025
18. Laskowsky, R. A., MacArthur, M. W., Moss, D. S., and Thornton, J. M. (1993) *J. Appl. Crystallogr.* **26,** 283–286
19. Dauter, Z., Dauter, M., and Dodson, E. (2002) *Acta Crystallogr. Sect. D Biol. Crystallogr.* **58,** 494–506
20. Holm, L., and Sander, C. (1993) *J. Mol. Biol.* **233,** 123–138
21. Harding, M. M. (2004) *Acta Crystallogr. Sect. D Biol. Crystallogr.* **60,** 849–859
22. Janda, I, D. Y., Derewanda, U, Dauter, Z, Bielicki, J, Cooper, D. R., Graf, P. C. F., Joachimiak, A, Jakob, U, and Derewanda, Z. S. (2004) *Structure* **12,** 1901–1907
23. Cameron, A. D., Ridderström, M., Olin, B., Karavana, M. J., Creighton, D. J., and Mannervik, B. (1999) *Biochemistry* **38,** 13480–13490
24. Board, P. G., Coggan, M., Chelvanayagam, G., Easteal, S., Jermiin, L. S., Schulte, G. K., Danley, D. E., Hoth, L. R., Griffor, M. C., Kamath, A. V., Rosner, M. H., Chrunyk, B. A., Perregaux, D. E., Gabel, C. A., Geoghegan, K. F., and Pandit, J. (2000) *J. Biol. Chem.* **275,** 24798–24806
25. Krezel, A., Wojcik, J., Maciejczyk, M., and Bal, W. (2003) *Chem. Commun.* (*Camb.*) 704–705
26. Jacob, C., Maret, W., and Vallee, B. L. (1998) *Proc. Natl. Acad. Sci. U. S. A.* **95,** 3489–3494
27. Jiang, L.-J., Maret, W., and Vallee, B. L. (1998) *Proc. Natl. Acad. Sci. U. S. A.* **95,** 3483–3488
28. Kruer, M., Haumann, M., Meyer-Klaucke, W., Thauer, R. K., and Dau, H. (2002) *Eur. J. Biochem.* **269,** 2117–2123
29. Evans, J. C., Huddler, D. P., Hilgers, M. T., Romanchuk, G., Matthews, R. G., and Ludwig, M. L. (2004) *Proc. Natl. Acad. Sci. U. S. A.* **101,** 3729–3736
30. Graumann, J. L., H., Tang, X., Tucker, K. A., Hoffmann, J. H., Vijayalakshmi, J., Saper, M., Bardwell, J. C., and Jakob, U. (2001) *Structure* (*Lond.*) **9,** 377–387
31. Won, H.-S., Low, L. Y, De Guzman, R., Martinez-Yamout, M., Jakob, U., and Dyson, H.J. (2004) *J. Mol. Biol.* **341,** 893–900
32. Kurek, I., Kawagoe, Y., Jacob-Wilk, D., Doblin, M., and Delmer, D. (2002) *Proc. Natl. Acad. Sci. U. S. A.* **99,** 11109–11114
33. Zou, M. H., Shi, C., and Cohen, R. A. (2002) *J. Clin. Investig.* **109,** 817–826